

Singlet exciton relaxation in isolated polydiacetylene chains studied by subpicosecond pump-probe experiments

B. Kraabel* and M. Joffre

Laboratoire d'Optique Appliquée, URA 1406 du CNRS, ENSTA-Ecole Polytechnique, F-91125 Palaiseau Cedex, France

C. Lapersonne-Meyer† and M. Schott‡

Groupe de Physique des Solides, UMR 75-88 du CNRS, Universités Paris 6 et 7, 2 Place Jussieu, F-75251 Paris Cedex 05, France

(Received 1 May 1998)

Singlet 1B_u exciton relaxation in polydiacetylene chains isolated in their crystalline monomer matrix is studied by subpicosecond pump-probe experiments. Results on photoinduced absorption (PA) and on 1B_u exciton absorption bleaching [photobleaching (PB)] are presented. It is shown that three excited states lie in the optical gap, apart from the triplet 3B_u exciton. Two short-lived states (respective lifetimes $\tau \approx 450$ fs and 2 ps) of very similar PA cross sections and PB efficiencies, belong to the same relaxation pathway. A third longer-lived state ($\tau \geq 30$ ps) is responsible for a slow PB component and exists independently of the triplet exciton, which has its own signature [B. Kraabel *et al.*, Chem. Phys. **227**, 83 (1998)]. There is a branching in the 1B_u exciton relaxation, excluding a single cascade of these three states. The proposed nonradiative relaxation scheme involves two A_g states. Self-trapping is also discussed and it is concluded that, if present, it cannot be instantaneous. Our data suggest that self-trapping is at best a minor component of the B_u singlet exciton relaxation in polydiacetylene isolated chains.

[S0163-1829(98)02744-1]

I. INTRODUCTION

Polydiacetylenes (PDA's) are good model systems for the study of conjugated polymers because they can be obtained as single crystals of macroscopic size by solid-state polymerization of the corresponding diacetylene (DA) crystal.¹⁻³ Such crystals are usually considered as a collection of one-dimensional (1D) chains, neglecting interchain interactions. However, studies on several conjugated polymers such as PPV have demonstrated the existence of interchain excitons, i.e., bound electron-hole pairs on neighboring chains.^{4,5} This brings into question the interpretation of the photophysics in PDA's in terms of isolated polymer chains.

We study here DA monomer single crystals containing chains of the corresponding polydiacetylene polymer at a concentration of approximately 10^{-4} in weight. The chosen DA's are known as 3BCMU and 4BCMU and have the side groups $-(\text{CH}_2)_n-\text{OCO}-\text{NH}-\text{COOC}_4\text{H}_9$, where $n=3$ for 3BCMU and $n=4$ for 4BCMU. Thermal polymerization of these DA's is negligible, so a small and constant polymer concentration can be maintained in a sample. However, they readily polymerize under γ -ray irradiation. The resulting chains are very long (2.6 μm in the case of PDA-4BCMU, with a very small dispersion in length⁶), and are thus good approximations of infinite chains. At a concentration $\approx 10^{-4}$ in weight the average interchain distance is several tens of nanometers. Thus interchain interactions can be neglected and each chain may be considered as an isolated 1D system. Moreover, in the crystalline monomer matrix, all the chains are perfectly aligned and parallel, with the same geometry and the same environment (surrounding monomer crystal). They are, in fact, 1D crystals.

Their absorption spectrum is dominated by an intense and

highly dichroic line (dichroic ratio ≥ 250), peaking at $\nu_0 = 14\,585\text{ cm}^{-1}$ ($\approx 1.81\text{ eV}$) in PDA-4BCMU and at $\nu_0 = 15\,330\text{ cm}^{-1}$ ($\approx 1.90\text{ eV}$) in PDA-3BCMU at 15 K. This transition corresponds to the lowest-lying 1B_u free exciton. For the sake of simplicity we refer to the 1B_u free exciton, and its transition energy, as ν_0 . The corresponding absorption line is very narrow at low temperature (fullwidth at half maximum 7.4 meV at 10 K) indicating that inhomogeneous broadening is very small, and giving a lower limit for the lifetime of ν_0 of $\tau_0 \geq 90$ fs.

Weak absorption lines appear on the low energy side of the absorption line at ν_0 . They correspond to excitons of very similar electronic properties, but located on different chains with slightly different ground-state conformations.^{7,8} These are further discussed in the Appendix.

Both the PDA-3 and -4BCMU chains isolated in their respective monomer matrices exhibit a weak fluorescence,^{8,9} whereas the bulk PDA-4BCMU is considered to be nonfluorescent. Apart from the region of the main exciton transition where emitted light is reabsorbed, the emission spectrum is essentially a mirror image of the exciton absorption with no Stokes shift. The emission origin coincides with the main exciton absorption energy to within the experimental accuracy of a few cm^{-1} . Since this fluorescence is weak, the free-exciton relaxation is dominated by nonradiative processes. Preliminary time-resolved luminescence measurements indicate a fluorescence lifetime $\tau_0 \leq 200$ fs.¹⁰

To our knowledge, the singlet exciton-relaxation scheme has never been studied before on isolated PDA chains and is investigated here through subpicosecond pump-probe experiments. The triplet exciton generation and relaxation processes have been studied using the same experimental method in our previous paper.¹¹ The important literature on

these processes in bulk PDA's Refs. 12–14 will not be reviewed here; instead, we briefly recall the facts relevant to the present paper.

In bulk form, PDA's are known to exist in two different electronic states, characterized by exciton transitions at 1.9–2 eV (the so-called “blue phase”), and ~ 2.4 eV (the “red phase”). The characteristic times observed during exciton relaxation are somewhat different in the two phases. The blue-phase materials that have been most studied are poly-PTS single crystals, polycrystalline PDA-4BCMU films, and cast PDA-3BCMU films; 1B_u exciton relaxation is very similar in all these systems. The electronic properties of the isolated chains in PDA-3BCMU and PDA-4BCMU studied here correspond to this phase.

The most complete model for exciton relaxation in PDA's has been proposed by Kobayashi and co-workers.^{14–16} It is based on a prediction of the theory of exciton self-trapping, which states that there is no barrier to self-trapping in one dimension.^{17–19} It is assumed that chains in PDA's behave as 1D systems for both electrons and phonons, at least in the relevant time range. The optically excited free exciton starts to evolve instantaneously, within a half period of the C=C stretching vibration (~ 20 fs), since electron-phonon coupling is very strong in PDA's. A “hot” self-trapped exciton (STE) is thus formed, which cools down in a fraction of a picosecond. The thermalized STE is converted back into the ground state with a lifetime of 2 ps, by tunneling to the ground-state potential energy curve. There is a single level in the optical gap, the STE. However, in more recent papers by the same authors, the possibility of the STE being an A_g state^{20(a)} or of an A_g state being involved in the relaxation scheme of the STE [Ref. 20(b)] is considered.

Our paper is organized as follows: The experimental methods are presented briefly in Sec. II. Photoinduced absorption and photobleaching results are presented in Sec. III and discussed in Sec. IV. It is shown that there are at least three excited states in the optical gap, two short lived (lifetimes ~ 0.45 and 2 ps) and one longer lived (~ 30 ps). The latter is distinct from the triplet state. The nature of these states is then discussed in comparison to data from the literature on blue-phase bulk PDA.

II. EXPERIMENTAL SETUP

The experimental setup used for this study has been described in detail in a previous paper.¹¹ It consists of a mode-locked Ti:sapphire oscillator amplified at a 250 kHz repetition rate, which produces 150 fs, 4 μ J pulses at 800 nm (Coherent RegA system). A portion of this output is split off and focused into a sapphire plate to form a single-filament continuum, which is then further split to serve as both the seed for an optical parametric amplifier (OPA) and the probe for a pump-probe experiment. The remaining power in the 800 nm pulse train is doubled and used to pump the OPA, thus producing a pulse train continuously tunable from 500 to nearly 800 nm. The tunable output of the OPA serves as the pump while the continuum serves as the probe in a conventional pump-probe experiment. The pump photon energy is always kept below the known electron-hole pair generation threshold.⁷ The accessible probe spectral range lies between 1.25 and 2.3 eV, but it is difficult to probe the spectral

region from 1.5 to 1.6 eV since this is near the strong peak in the continuum spectrum at the fundamental wavelength of 800 nm. We measure the differential absorption as a function of delay time between the pump and probe pulse, and, for a given delay time, as a function of the intensity of the pump pulse.

After passing through the sample, the continuum probe pulses are dispersed in a single-grating spectrometer and the spectrum is focussed onto a liquid nitrogen cooled charge-coupled device detector. The probe spectrum is measured with and without the pump (I_{on} and I_{off} , respectively) at a 12 Hz repetition rate, which yields (in the small signal limit in which we generally operate) the differential absorption signal, $-\Delta\alpha d = \ln[I_{\text{on}}(\omega)/I_{\text{off}}(\omega)]$. Although the signal-to-noise ratio achievable using this method is less than what can be achieved using a monochromator and synchronous, phase-sensitive, differentially amplified detection,²¹ the rapid collection of the entire spectrum at each delay time is crucial for this experiment for several reasons. Because the bleaching of the ground-state absorption reveals sharp (width 10–20 meV) excitonic bands it is necessary to fit these in their entirety in order to accurately measure the dynamics of the recovery of the ground state. This avoids possible systematic errors due to changes in the position and/or linewidth of the bleached line. Using single-channel detection would preclude detection of these effects, and, if they were present, they would manifest themselves by altering the measured dynamics in a systematic way. In addition, the bleached absorption bands are superimposed over a broad-band photoinduced absorption (PA), so that accurate fitting of the bleached line shape is crucial in order to separate the time dynamics of the bleaching from that of the PA.

The probe pulses obtained through continuum generation are strongly chirped. They were carefully characterized over the entire spectral range using two-photon absorption in a GaSe crystal.²² Considering the extremely broad spectral range of the probe, chirp compression was considered impractical. The frequency-domain data we present are raw experimental results, i.e., not corrected for chirp. Hence, the different frequency components do not correspond to the same pump-probe time delay. However, the time-domain data shown have been corrected for the known value of the chirp, and therefore can be directly compared with each other. Because the various differential absorption bands [PA or photobleaching (PB)] have a bandwidth typically between 10 and 20 meV, we note that the amount of chirp in the visible over a bandwidth of this size causes a maximum of 20 fs group delay between the different spectral components of the probe pulse. This is much smaller than the 150 fs pulse width, and therefore can be safely neglected when fitting to the lineshape of a differential absorption band.

Another issue that must be considered is the possible occurrence of the so-called spectral oscillation artefact, which has been observed in the dynamics of exciton lines when the dephasing time is much longer than the pump-pulse duration.²³ However, in the present experiments the dephasing time is at most 200 fs comparable to the pump duration, so that coherent effects are expected to be much smaller. Indeed, we performed a careful numerical calculation and found that, in our experimental conditions, coherent effects cause only minor changes in the differential absorption spec-

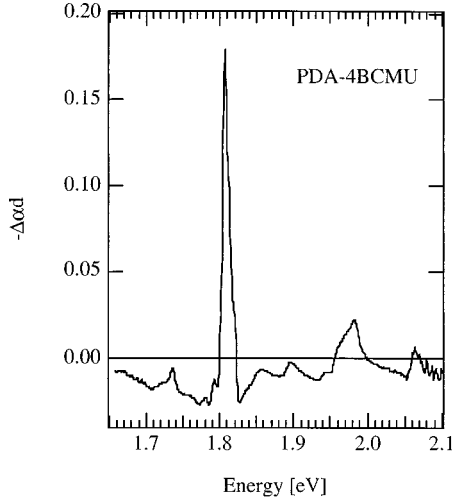


FIG. 1. Differential absorption of PDA-4BCMU chains isolated in 4BCMU monomer matrix, at a delay time of 1 ps (at 1.81 eV). The spectrum is not corrected for the chirp of the probe pulse.

trum in the immediate vicinity of the exciton absorption line. Furthermore, the artefact is present only when the pump and probe pulses overlap. Finally, the effect is even less important in the case of time-domain data. Therefore, we are confident that this artefact plays no significant role in the experimental results reported below.

Single crystals of monomer 3BCMU and 4BCMU are grown by slow evaporation of saturated solutions of freshly recrystallized monomer in acetone or methylisobutylketone at 4 °C in the dark. The crystals are plate shaped, with an area of 0.1–1 cm², and a thickness of 50–250 μm. They contain a very small amount of polymer chains dispersed in the crystalline monomer matrix, $x_p = 10^{-5} - 10^{-4}$ in weight. Controlled amounts of polymer can be generated by irradiation with low γ -ray doses.⁶

III. EXPERIMENTAL RESULTS

The pump photons can generate several types of excited states, and the overall absorption spectrum is modified in two ways: (1) PB, which is the decrease of absorption by the ground state partially depopulated by the pump, and (2) PA, which is the generation of new absorption bands corresponding to the excited states created by the pump.

Since we pump below the known electron-hole generation gap,⁷ the pump photons cannot generate charge carriers. Hence, only exciton states contribute to the differential absorption.

Figure 1 shows the differential absorption spectrum between 1.6 and 2.1 eV of an optically thin sample of PDA-4BCMU at a delay time of 1 ps at ν_0 . In this figure, as well as in all those in which PB peaks appear, the negative differential absorption is plotted, so that the PB appears as narrow positive peaks similar to the linear absorption spectrum, and the PA appears as broad negative bands. A similar spectrum is obtained on PDA-3BCMU.

The PB kinetics is that of the ground-state repopulation in which all excited states are involved, whereas each excited state has its own PA. If a spectral range may be found where only one excited state absorbs, the kinetics of this PA is then

that of the corresponding excited-state population (in the small-signal limit). It is then potentially easier to account for the PA results, and these will be presented first.

A. Photoinduced absorptions

Three spectral ranges have been studied, in which different PA kinetics are observed. The two materials studied (PDA-3BCMU and -4BCMU) show very similar results in all three spectral ranges. The PA kinetics are obtained by averaging over a 10 meV bandwidth centered at the given energy.

In order to fit the kinetics we use the following formalism. As will be shown below, we find it necessary to introduce two intermediate states below ν_0 , which are referred to as X_1 and X_2 . The population of the various excited states is then modeled by numerically integrating the following rate equations:

$$\frac{dn_{\nu_0}(t)}{dt} = \left(\frac{\sigma_g(\omega_{pp})I_{pp}(t)}{h\omega_{pp}} \right) [n_g(t) - n_{\nu_0}(t)] - \frac{n_{\nu_0}(t)}{\tau_0}, \quad (1a)$$

$$\frac{dn_{x_1}(t)}{dt} = \frac{n_{\nu_0}(t)}{\tau_0} - \frac{n_{x_1}(t)}{\tau_1}, \quad (1b)$$

$$\frac{dn_{x_2}(t)}{dt} = \frac{n_{x_1}(t)}{\tau_1} - \frac{n_{x_2}(t)}{\tau_2}, \quad (1c)$$

$$n_0 = n_g + n_{\nu_0} + n_{x_1} + n_{x_2}. \quad (1d)$$

In these equations $\sigma_g(\omega_{pp})$ and n_g refer to the ground-state absorption cross section and population density, respectively, n_i and τ_i refer to the population density and lifetime of state i , respectively, and $I_{pp}(t)$ represents the pump flux. The saturation density is given by the constant term n_0 . In order to calculate the PA signal, we take the convolution of the population densities with the probe pulse,

$$\Delta\alpha(t, \omega_{pb}) \propto \int_{-\infty}^{\infty} dt' I_{pb}(t' - t) [\sigma_{\nu_0}(\omega_{pb})n_{\nu_0}(t') + \sigma_{x_1}(\omega_{pb})n_{x_1}(t') + \sigma_{x_2}(\omega_{pb})n_{x_2}(t')], \quad (2)$$

where $\sigma_i(\omega_{pb})$ represents the absorption cross section of state i at frequency ω_{pb} , and $I_{pb}(t)$ represents the probe flux. We use a $\text{sech}^2(2.269/\tau_i)$ pulse shape for both the pump and probe pulse, with $\tau_{pp} = 150$ fs for the pump pulse and $150 < \tau_{pb} < 220$ fs for the probe pulse, depending on the wavelength of the spectral region under consideration.

1. Near-IR region (1.2–1.45 eV)

A typical PA spectrum in the near IR (NIR) is shown in Fig. 2. At delay times less than 1 ps, the spectrum has two components, an intense and narrow Lorentzian line peaking at ≈ 1.35 eV, which is superimposed on a shorter lived, broad-band component.

This broad band disappears within a few ps of the pump pulse, leaving only the narrow Lorentzian absorption line. This line is the TT^* photoinduced absorption, and by monitoring it the triplet population can be studied. Results on

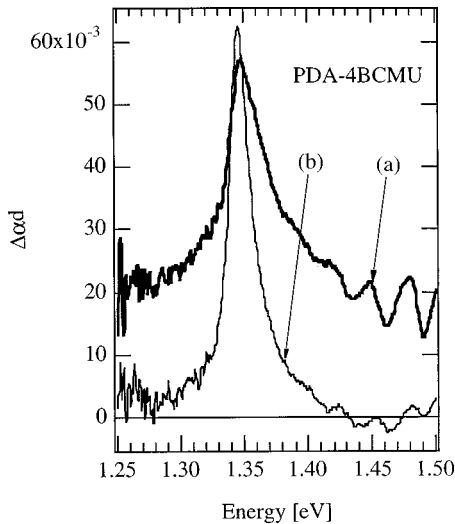


FIG. 2. Near-infrared-photoinduced absorption spectra of PDA-4BCMU chains. Spectrum (a) is at a delay time of 335 fs and spectrum (b) is at 1.3 ps. Spectra are not corrected for chirp of the probe pulse; the delay times given are for 1.35 eV.

triplet exciton generation, transport, and relaxation are presented and discussed in a separate paper.¹¹ In the present paper, only the short-lived component is of interest in connection with the singlet exciton dynamics.

It is seen from Fig. 2 (spectrum a) that the threshold of this structureless band is probably below 1.2 eV, beyond our accessible spectral range. Its time dependence is shown in Fig. 3. The rise time is that of the pump pulse. The decay can be measured over one order of magnitude. It is initially exponential with a lifetime $\tau_1 = 450 \pm 100$ fs independent of the probe wavelength in the NIR domain, and of the pump fluence and wavelength. In what follows, the state with lifetime τ_1 will be referred to as X_1 . The dispersion on the fitted

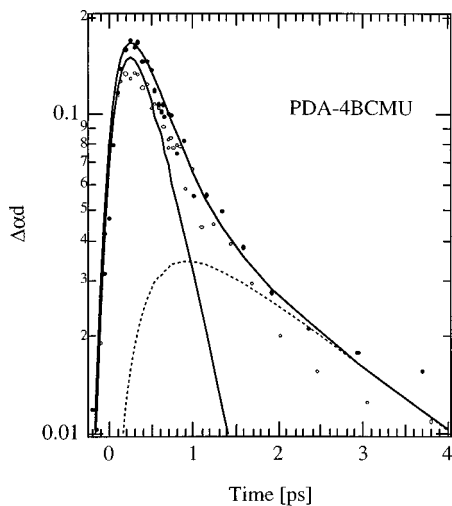


FIG. 3. Time dependence at 1.45 eV (solid circles) and 1.29 eV (open circles) of PDA-4BCMU, corrected for the chirp of the probe pulse. The heavy solid line is a fit using Eq. (2) with $\sigma_{\nu_0} : \sigma_{x_1} : \sigma_{x_2} = 7 : 1$. The thin solid line shows the contribution of the state X_1 , with $\tau_1 \approx 450$ fs. The dashed line shows the contribution of the state X_2 with $\tau_2 \approx 2$ ps.

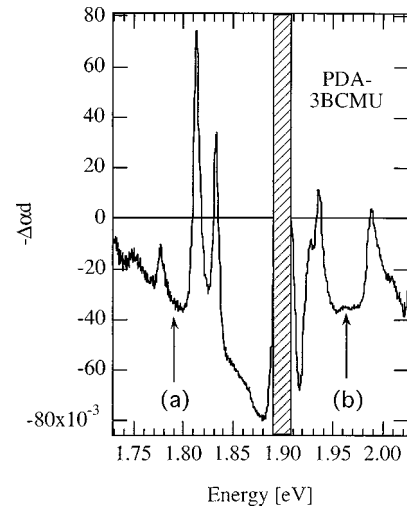


FIG. 4. Differential absorption of PDA-3BCMU chains in the spectral region near ν_0 . The hatched region corresponds to total absorption by ν_0 , where the differential absorption cannot be measured. The kinetics of the PA's shown in Fig. 5 were determined by averaging over 10 meV bands about (a) 1.79 and (b) 1.965 eV (see arrows).

values of τ_1 is experimental, since the signal-to-noise ratio becomes poor beyond the first ps.

A weaker and longer-lived PA component is present in the ps time range, but is too small to be analyzed directly. However, in order to achieve the best fit for the short-lived component, it is necessary to assume that this longer-lived component has the same lifetime ($\tau_2 \approx 2$ ps) as found in the PA and PB in the visible region. The state of lifetime τ_2 will be referred to as state X_2 and will be discussed more below.

Thus, we use Eq. (2), with $\tau_2 = 2$ ps and $\tau_0 < 200$ fs in Eq. (1) to fit to the kinetics shown in Fig. 3. The result, shown as the thick solid line in Fig. 3, yields $\sigma_{\nu_0} : \sigma_{x_1} : \sigma_{x_2} = 0 : 7 : 1$ for this spectral region. The same results are obtained on PDA-3BCMU at 20 and 77 K and PDA-4BCMU at 20 K.

The absolute cross section for absorption can be estimated using the relation

$$\sigma = \frac{\{\Delta\alpha d\}}{d_{\text{eff}}} \frac{1}{n} \quad \text{with} \quad n = \frac{\rho x_p N_A \delta}{Mm}, \quad (3)$$

where $\{\Delta\alpha d\}$ is the measured differential absorption, d_{eff} is the sample thickness, ρ is the sample density, x_p is the weight fraction of polymerization, N_A is Avogadro's number, M is the polymer repeat unit molecular weight in Dalton, m is the number of monomers per photon absorbed, and δ is the number of excitations of type X_1 created per photon absorbed. Equations (1) imply $\delta = 1$ (this is further discussed in Sec. IV B below). Using $\rho = 1.22$ g/cm³, $x_p = 10^{-4}$, $M = 508$ g/mol, $m = 100$, and the experimental values of $d_{\text{eff}} = 150$ μm and $\{\Delta\alpha d\} = 0.01$ gives $\sigma \approx 3 \times 10^{-16}$ cm² for the range 1.5–1.2 eV. This is an intense transition with an oscillator strength of order 1.

2. Visible region

Figure 4 shows the experimental differential absorption of PDA-3BCMU chains in the region around the exciton peak at ν_0 . We purposefully used a sample with a higher polymer content in order to record more accurate differential absorp-

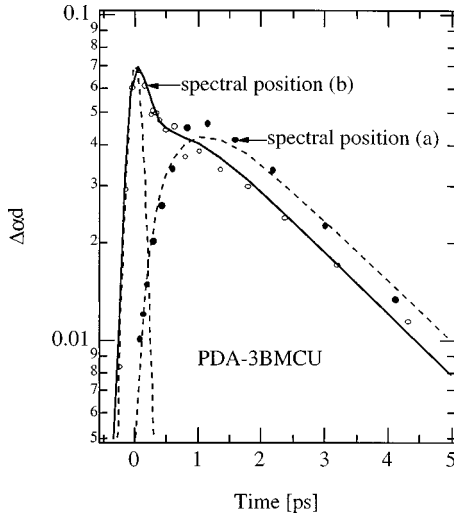


FIG. 5. Time dependence of the PA at 1.965 eV (open circles) and 1.79 eV (solid circles), corrected for the chirp of the probe pulse. The heavy solid line is a fit using Eq. (2) with $\sigma_{\nu_0}:\sigma_{x_1}:\sigma_{x_2} = 5:1:2$. The thick dashed line is the (scaled) result of setting both σ_{ν_0} and σ_{x_1} equal to zero, leaving only the contribution from state X_2 . The thin dotted line is the cross correlation of the pump pulse (150 fs) and the probe pulse at 1.965 eV (200 fs).

tion spectra in this spectral region. This sample thus absorbs so strongly at ν_0 that it was impossible to measure the differential absorption there, hence the corresponding spectral region is hatched on Fig. 4. Narrow PB lines corresponding to the vibronic replicas of ν_0 , and also to ν_a , ν_b , and ν_c (see the Appendix), appear at the same positions as the absorption lines in the linear-absorption spectrum. Between these PB peaks, spectral regions exist where the differential absorption is positive; that is PA is dominant. The behavior of this PA is different below and above the energy ν_0 .

The singlet 1B_u exciton energy ν_0 at 20 K is not precisely the same for the two materials: 1.9 eV for PDA-3BCMU and 1.8 eV for PDA-4BCMU. Since our experimentally accessible-probe energy range starts around 1.6 eV, the spectral region below ν_0 where PA can be studied is wider in PDA-3BCMU. Thus, this material has been chosen for the experimental study but it was verified that results on PDA-4BCMU are similar.

In the visible range below ν_0 , the PA band is broad and structureless (several sharp bleaching features can be seen below ν_0 ; these will be discussed in the Appendix). Above ν_0 , bleaching of the vibronic replicas of ν_0 can be seen, superimposed on a broad PA background. Figure 5 shows the dynamics obtained by averaging over a 10 meV band centered at the spectral positions denoted by the arrows in Fig. 4. The open circles show the dynamics at 1.965 eV [spectral position (b)], above the energy ν_0 . The heavy solid line shows the result of using Eq. (2) to fit the data, from which we obtain $\sigma_{\nu_0}:\sigma_{x_1}:\sigma_{x_2} = 5:1:2$, $\tau_0 < 200$ fs, $\tau_1 = 450 \pm 100$ fs and $\tau_2 = 2 \pm 0.3$ ps. The solid circles in Fig. 5 show the kinetics at 1.79 eV [spectral position (a)], corrected for the chirp of the probe pulse so that the time origin for both spectral positions (a) and (b) coincide. The kinetics of the PA below ν_0 are similar in the spectral range between 1.6 eV and ν_0 . We obtain an excellent fit to the kinetics at (b) simply by setting $\sigma_{\nu_0} = \sigma_{x_1} = 0$ in the fit used for the kinetics

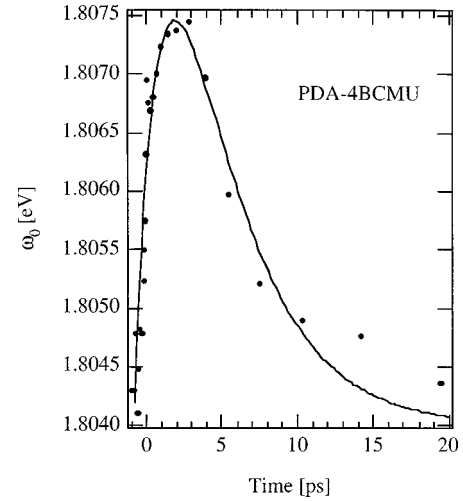


FIG. 6. Time dependence of the resonance energy of the PB peak of ν_0 upon pumping at 2 eV with an excitation density of one photon absorbed every 70 monomer repeat units. The blueshift of the resonance is fit to a monoexponential with a time constant of 600 fs, while the redshift is fit to monoexponential with a time constant of 4 ps. The time origin corresponds to the maximum of the PB magnitude.

at (a) (and scaling the result), implying that the state X_2 is indeed populated from state X_1 .

Using Eq. (3), with $\delta=1$ and $\Delta\alpha d=0.02$ we estimate the cross section for absorption by the species X_2 to be $\sigma_{x_2} \approx 8 \times 10^{-16}$ cm² in the range between ν_0 and 1.6 eV. This again is a large value corresponding to an oscillator strength of order unity. States X_1 and X_2 thus have comparable absorption spectra, their respective thresholds being separated by ~ 0.4 eV.

The final state or states of these PA transitions should be about 3 eV above ground state. If X_1 and X_2 are A_g states as discussed below, these final states should be of B_u symmetry and connected to the ground state by an allowed transition. The valence to the conduction band threshold in isolated PDA chains is around 2.4 eV,⁷ and the bands are broad, but the corresponding oscillator strength is small. The most likely candidate for a final state would then be an exciton state resonant with the continuum, and the corresponding absorption would be broad, as are the PA spectra. There is indeed a broad absorption plateau near 3 eV but this is a subject for further study.

B. Photobleaching of main exciton

1. Spectrum and kinetics

The overall transient PB spectrum (Figs. 1 and 4) looks very similar to the linear absorption spectrum. The position of the PB peaks are almost constant in time and equal to those of the corresponding absorption peaks during the entire decay. The position of the peak at ν_0 was accurately measured, showing a slight blue shift by ~ 3 meV (less than 30% of the peak width), within about 1 ps. The peak returns to its initial position with a time constant of about 4 ps (Fig. 6). Thus, the effect is a very minor one, and cannot be taken as evidence of spectral relaxation. The shift might be associated with the generation and decay of a large phonon population consecutive to electronic energy relaxation on the chain.

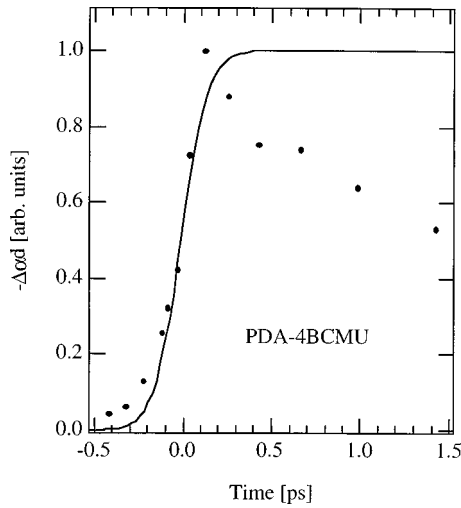


FIG. 7. Early time dynamics of the PB of ν_0 in PDA-4BCMU upon pumping at 2.00 eV at an excitation density of one photoexcitation every 150 monomer repeat units. The thin line shows the convolution of the integral of a 150 fs pump pulse with a 150 fs probe pulse.

At the wavelengths corresponding to peaks in the differential absorption spectrum (ν_0 and its two main vibronic replicas) PB dominates (Figs. 1 and 4). To obtain the kinetics of the PB we first fit the low-energy side of the PB peak with a Gaussian. The data shown for the kinetics is the magnitude of these Gaussian fits. For PDA-3BCMU and -4BCMU the kinetics of the photobleaching of the main exciton and the double and triple bond vibronic replicas are identical for all pump wavelengths used. For PDA-3BCMU the PB signal appears instantaneously within the pump-pulse duration for pump wavelengths from 1.9 to 2.4 eV. For PDA-4BCMU the same is true for pump wavelengths from 1.8 to 2.1 eV. This is shown in Fig. 7 for the case of PDA-3BCMU. However, slight differences exist between the two materials at very early times, ≤ 1.5 ps which will be discussed below.

For PDA-4BCMU, as seen in Fig. 8, the whole time decay of the PB at ν_0 up to the longest time studied (~ 50 ps) is well described by a sum of two exponentials with lifetimes 1.7 ± 0.2 ps and 30–40 ps, except the first few points ($t \leq 0.5$ ps, see inset), which are slightly above the fit, indicating a faster initial decay. The long lifetime is very poorly determined since it can be followed over a small dynamic range only. The long-time component has a zero time extrapolated ordinate of ~ 0.1 relative to the short-time component. This ratio stays constant to within 15% in all experimental conditions; i.e., whatever the pump fluence and wavelength (see discussion below).

In PDA-3BCMU, the decay beyond ~ 1.5 ps is also fitted (Fig. 9) by a sum of two exponentials with time constants and relative intensities similar to those in PDA-4BCMU. It is only between 0 and 1.5 ps (see inset in Fig. 9) that differences with PDA-4BCMU are observed. In this time range the decay has a kind of S shape, initially faster, then slower, than the 2 ps time constant exponential. It was checked that this fast initial decay is not a coherence artefact (see Sec. II). This decay is further analyzed in Sec. IV D.

2. Bleaching efficiency

The initial differential absorption at ν_0 , $\Delta\alpha_0(\nu_0)$, is mainly due to bleaching of the exciton absorption. The ratio

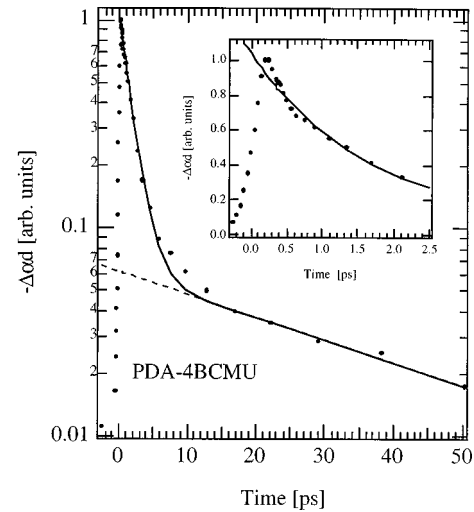


FIG. 8. Dynamics of the PB of ν_0 in PDA-4BCMU upon pumping at 2.07 eV at an excitation density of one photoexcitation every 300 monomer repeat units. The thin solid line is a double exponential fit with time constants $\tau_2 = 1.65$ ps and $\tau_3 = 40$ ps. The thin dashed line shows the contribution of the long-lived component extrapolated to time zero. The inset shows the early time dynamics with the double exponential fit on a linear scale.

of $\Delta\alpha_0(\nu_0)$ to the absorbance $\alpha(\nu_0)$ of the sample at the same wavelength yields the fraction of the monomer units of chains present in the crystal that are bleached, i.e., “removed” by the electronic excitations generated by the pump. Since the absorbance of the sample at the pump wavelength and the pump fluence are known, the number of generated excitations can be calculated. The bleaching efficiency ϕ_i (where the subscript i refers to the state under consideration) of such an excitation is then expressed as the number of monomer units that are bleached per excitation generated.

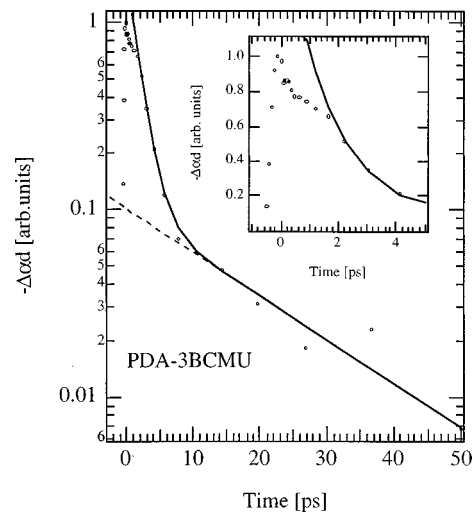


FIG. 9. Dynamics of the PB of the vibronic replica of ν_0 (1.99 eV) in PDA-3BCMU upon pumping at 2.07 eV with an excitation density of one photoexcitation every 100 monomer repeat units. The thin solid line is a double exponential fit with time constants $\tau_2 = 1.7$ ps and $\tau_3 = 20$ ps and the thin dashed line shows the contribution of the long-lived component extrapolated to time zero. The inset shows the early time dynamics and the double exponential fit on a linear scale.

The bleaching efficiency ϕ_{ν_0} of the initial exciton is estimated in our samples to be ~ 5 monomer units, corresponding to a length of ~ 25 Å on a chain. The bleaching efficiency of the states X_1 and X_2 can then be determined relative to that of ν_0 by fitting the PB kinetics using Eqs. (1) and (2) (in a slightly modified form). This is done in Sec. IV B; for now it suffices to note simply that the bleaching efficiencies of states X_1 and X_2 are not drastically different, since the PB decays smoothly with no dramatic discontinuities as might be expected if one state had a much smaller or larger bleaching efficiency than its predecessor.

IV. DISCUSSION: RELAXATION OF THE FREE EXCITON

Though excitonic states ν_a , ν_b (and ν_c in PDA-3BCMU) appear in the absorption and photobleaching spectra as distinct lines below the main exciton absorption energy, they play no part in the relaxation process of the free-exciton state. Indeed, photobleaching experiments clearly show that no coupling exists between states ν_0 , ν_a , ν_b , and ν_c (see the Appendix). All spectra—absorption, electroabsorption, photobleaching, and emission—must be taken as the sum of individual spectra each corresponding to a given chain population. The dominant one corresponds to the exciton absorption at ν_0 . The discussion here concerns the relaxation of this exciton.

A. Two short-lived states in the gap

From the PA results, two characteristic times τ_1 (≈ 450 fs) and τ_2 (≈ 2 ps) were found, indicating two electronic states apart from the free exciton at ν_0 whose lifetime is known to be ≤ 200 fs.¹⁰ These states are referred to as X_1 and X_2 , respectively. Our PA results give a rough idea of their respective absorption bands in the spectral range accessible to us. In the NIR (1.2 to 1.5 eV), state X_1 absorbs, with a small contribution from state X_2 . Note, however, that a contribution of the exciton at ν_0 to the observed PA cannot be excluded. With our time resolution, PA's from both X_1 and ν_0 would show the same instantaneous rise time, but absorption by ν_0 alone would approximately follow the pump-pulse temporal profile. In the visible region (1.65 to 1.9 eV), state X_2 of lifetime τ_2 absorbs and we observe its population from X_1 since τ_1 appears as the rise time. Above ν_0 , an instantaneous rise time is again observed, followed by an initial rapid decay, indicating that absorption by the exciton at ν_0 contributes in this spectral range. Furthermore, the fit using Eq. (2) implies that both states X_1 and X_2 contribute as well to the PA kinetics at this energy. From the fit we find the relative magnitude of the absorption cross sections to be $\sigma_{\nu_0}:\sigma_{x_1}:\sigma_{x_2}=5:1:2$ at this energy.

B. Another, longer-lived, state in the gap

A third decay time τ_3 (≈ 30 ps) is needed to fit the slow component observed in the PB decay kinetics. This implies that another state, referred to here as Y with a long lifetime is involved in the relaxation scheme. The question arises as to whether we have a single relaxation channel with all these states in series $\nu_0 \mapsto X_1 \mapsto X_2 \mapsto Y \mapsto S_0$, or whether there is a

branching from a certain level so that the state Y decays in parallel with the other state(s).

For the sake of simplicity, we shall discuss only two excited states X_2 and Y , neglecting the shorter-lived state X_1 which, as mentioned above, presents a PB efficiency comparable to that of X_2 . If the two states belong to the same relaxation channel according to $\mapsto X_2 \mapsto Y \mapsto S_0$, the photobleaching time dependence $B(t)$ is given by

$$B(t) = \phi_{x_2} n_{x_2}(t) + \phi_y n_y(t), \quad (4)$$

in which n_{x_2} and n_y are given by

$$n_{x_2}(t) = n_{x_2}(0) \exp(-t/\tau_2), \quad (5a)$$

$$n_y(t) = n_{x_2}(0) \left\{ \tau_2 / (\tau_y - \tau_2) \right\} \left\{ \exp(-t/\tau_2) - \exp(-t/\tau_3) \right\}, \quad (5b)$$

where τ_3 is the lifetime of state Y . As described in Sec. III B, the observed PB kinetics are well fitted by the sum of two exponentials with respective decay times τ_2 (≈ 2 ps) and τ_3 (≈ 30 ps), and the ratio of the zero time values of these exponentials is 10 ± 2 in all experiments. Equation (4) will describe the experimental decay provided the quantity

$$(\phi_{x_2}/\phi_y)(1 - \tau_2/\tau_3) - 1 \approx 10 \quad (6)$$

to account for a sum of two exponentials with a zero time-ordinate ratio ~ 10 . Using the experimental values of τ_2 and τ_3 , the ratio of respective bleaching efficiencies of states X_2 and Y should then be ~ 12 .

This seems unphysically large. In a very simple model, the bleaching efficiency of the initially present state is comparable to the extension of the wave function of the relevant state, i.e., its ‘‘size.’’ It is close to the value of 33 Å inferred by Greene *et al.* in poly-PTS single crystal, from transient reflectivity measurements.²⁴ The size of the free exciton in isolated chains of PDA-3BCMU and -4BCMU has been deduced from electroabsorption measurements as ~ 25 Å.⁷ Theoretical calculations by Suhai²⁵ on the same material also yield a similar size. Our temporal resolution is of the order of the free-exciton lifetime, but the initial decay of the bleaching has a much longer time constant. Therefore, the state(s) responsible for this initial bleaching has (have) an efficiency very close to the one expected for the free exciton, and presumably comparable extensions on the chain. It does not seem reasonable to assume that ϕ_y is significantly less than 1 (in monomer units). Thus, ϕ_{x_2} should be ≥ 12 ; i.e., a PB efficiency over twice that of the free exciton.

No such difficulty arises if a branching occurs from some level in the relaxation cascade. If, for instance, Y is formed from ν_0 in competition with X_1 and X_2 , and both Y and X_2 decay independently to the ground state with time constants τ_2 and τ_3 , then

$$B(t) = \phi_{x_2} n_2(0) \exp(-t/\tau_2) + \phi_y n_y(0) \exp(-t/\tau_3) \quad (7)$$

and a large zero time ordinate value just corresponds to a branching ratio $\eta = n_y(0)/n_2(0)$ favoring state X_2 .

Small differences between the PB efficiencies can explain the short time shape of the PDA-3BCMU and -4BCMU PB decays (Fig. 10). The fit is made using Eqs. (1) modified to take into account the existence of state Y , as follows:

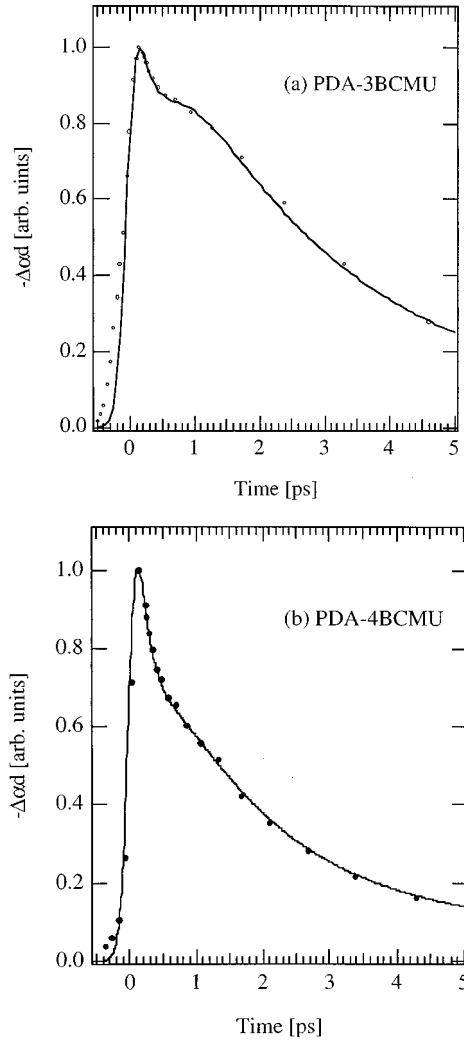


FIG. 10. Early time dynamics of the PB at ν_0 in PDA-3BCMU (a) and PDA-4BCMU (b) upon pumping at 2.07 eV with an excitation density of one photoexcitation every 100 monomer units. The thin line is a fit using Eq. (2) as described in the text.

$$\frac{dn_{\nu_0}(t)}{dt} = \left(\frac{\sigma_g(\omega_{pp})I_{pp}(t)}{h\omega_{pp}} \right) [n_g(t) - n_{\nu_0}(t)] - \frac{n_{\nu_0}(t)}{\tau_0}, \quad (1a)$$

$$\frac{dn_{x_1}(t)}{dt} = \delta \frac{n_{\nu_0}(t)}{\tau_0} - \frac{n_{x_1}(t)}{\tau_1}, \quad (1b')$$

$$\frac{dn_{x_2}(t)}{dt} = \frac{n_{x_1}(t)}{\tau_1} - \frac{n_{x_2}(t)}{\tau_2}, \quad (1c)$$

$$\frac{dn_y(t)}{dt} = (1 - \delta) \frac{n_{\nu_0}(t)}{\tau_0} - \frac{n_y(t)}{\tau_3}, \quad (1e)$$

$$n_0 = n_g + n_{\nu_0} + n_{x_1} + n_{x_2} + n_y. \quad (1d')$$

Replacing the absorption cross sections σ_i in Eq. (2) by the PB efficiencies ϕ_i , we can fit the early time PB kinetics to obtain the relative magnitude of the PB efficiencies ϕ_i . The results are shown in Fig. 10 and yield $\phi_{\nu_0}:\phi_{x_1}:\phi_{x_2} = 5:2.5:1$ for PDA-3BCMU and $\phi_{\nu_0}:\phi_{x_1}:\phi_{x_2} = 5:2.5:2.5$

for PDA-4BCMU. Since these fits are over a very small range, the results are not to be taken as definitive, but only as suggestive.

A similar conclusion follows if we assume Y is populated from X_1 . Since Y accounts for only $\sim 10\%$ of the total PB at short times, the two situations cannot be separated in our experiments.

It is also possible that the branching occurs in the decay of X_2 , the major channel being the nonradiative decay to the ground state and a minor one leading to Y , the branching ratio η being $\ll 1$. In the latter case, the population of Y would appear with a rise time of 2 ps, which is never observed in the PA. However, since the Y states are lower in concentration at short time than X_1 and X_2 , their contribution to PA is always a minor one. Indeed, in the visible range, a very small PA, a few percent of the peak value, persists at long times and seems to decay on a time scale longer than 10 ps. This may be PA by Y , but the poor signal-to-noise ratio prevents further study of it.

Assuming that the PB efficiency of the Y state is not larger than that of X_1 and X_2 , i.e., 2–3 monomer units, and not smaller than one monomer unit, the branching ratio η [$\eta = (1 - \delta)/\delta$] is $0.1 \leq \eta \leq 0.3$. This enables us to evaluate the rate constant k_Y for Y formation. For instance, if Y is formed from ν_0 , $k_Y \sim 1 \pm 0.5 \times 10^{12} \text{ sec}^{-1}$. If it is formed from X_1 , $k_Y = 3 \pm 2 \times 10^{11} \text{ sec}^{-1}$, and from X_2 , $k_Y \sim 8 \pm 4 \times 10^{10} \text{ sec}^{-1}$.

C. Role of the triplet state

Since in the present experiments triplet excitons are formed as correlated triplet pairs by ‘hot’ singlet fission, and since these pairs annihilate by fusion on a time scale of ~ 30 ps,¹¹ the triplet state is a possible candidate for Y . However, the experimental temporal decays of the long-lived component of PB and of the TT^* PA line at ≈ 1.35 eV are not exactly the same, suggesting that Y and T might be different states. A convincing argument is given by the fact that the slow component of PB is always $\sim 0.1 \pm 0.02$ of the total zero time PB, whatever the pump photon energy, whereas the triplet yield upon pumping at the exciton energy ν_0 is ~ 50 times smaller than when pumping at higher energies, above the exciton fission threshold of ~ 2 eV.¹¹ In addition, the Y state is generated via a one-quantum process, since it is observed to be linear in pump regardless of the pump wavelength. This is also in contradiction with the observed intensity dependence of the triplet state, which is superlinear in pump fluence for all pump wavelengths used.

Moreover, if the slow PB component were due to the triplet population, this would imply a fission probability of at least 10%, assuming that the triplet PB efficiency is not significantly larger than that of the singlet. Such a fission yield would be very large indeed, being two orders of magnitude larger than the experimental yield found in a polycrystalline film of the PDA poly(1,6-bis(Ncarbazolyl)-2,4hexadiyne) (DCH).²⁰

We thus conclude that Y and T are different states.

Still, the triplet state must contribute to the PB. This contribution should be undetectable when pumping at ν_0 , where the triplet yield is small, and more important when pumping at higher energies. Since the zero time-ordinate ratio of the slow and fast components of the PB is the same in the two cases within the experimental uncertainties of about 20%, the

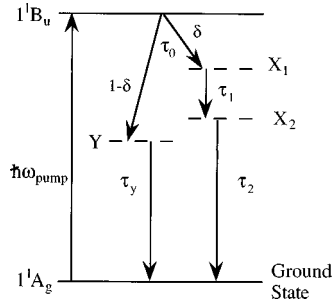


FIG. 11. Schematic diagram of the relaxation pathway for the 1B_u exciton. Only the time constants are meaningful in this figure, not the absolute energy positions of the levels, which are not known.

triplet contribution to PB cannot be larger than about 1%, giving for the fission yield an upper limit $\leq 1\%$, which is consistent with the DCH value.²⁶

D. Nature of the intermediate states

The free-exciton relaxation in bulk PDA's has generally been discussed in terms of only one intermediate state, a self-trapped exciton of B_u (Ref. 14) or A_g (Ref. 20) symmetry. Our results on isolated chains show that, apart from the triplet state, there are at least three excited states in the optical gap, but the assignment of these states is still speculative since they are characterized primarily by their respective lifetimes.

It has been shown that states X_1 and X_2 have comparable PB efficiencies, slightly smaller than that of the free exciton. They cannot be of B_u symmetry, since there is no evidence in any of our experiments on isolated PDA chains of any lower-lying B_u excited state accessible from the ground state. Linear absorption experiments on bulk PDA's also lead to absorption coefficients in the optical gap that are $\leq 1 \text{ cm}^{-1}$ except for weak vibrational overtone absorptions. However, two photon-absorption experiments on bulk PDA's have shown the existence of an A_g excited state in the optical gap, typically 0.2 eV below the B_u state.²⁷ There is even one report of the presence of two A_g states in the gap.²⁸

Our tentative interpretation is then to assign X_1 to an A_g state and Y to a self-trapped exciton formed from the free B_u exciton as sketched in Fig. 11. This requires that the $B_u \rightarrow A_g$ internal conversion rate constant is $\sim 5 \times 10^{12} \text{ sec}^{-1}$ since the B_u free exciton lifetime is $\leq 200 \text{ fs}$ and the predominant relaxation channel is towards X_1 . Such a rate constant is not unreasonably large considering what is known about polyenes.²⁹⁻³¹ This scheme also implies that self-trapping (Y state) is not instantaneous, since then $k_y \sim 1 \pm 0.5 \times 10^{12} \text{ sec}^{-1}$ (see Sec. IV B).

In the proposed scheme, X_1 is a free A_g exciton not too far below the 1B_u state. One would expect to see fluorescence from such a state as found in polyenes.³² Such a fluorescence is not observed here (nor in bulk PDA's). Its absence may be explained by the existence of a lower-lying state X_2 . This may be another free A_g exciton, making X_2 the 2A_g and X_1 the 3A_g state. Theoretical studies lead to the prediction of more than one A_g excited state below the 1B_u exciton if correlations are large enough,^{33,34} and there is experimental evidence for several A_g states in the two-photon

absorption spectrum of Lawrence *et al.* of poly-PTS.²⁸ A possibility that cannot be excluded at the present stage is that X_1 is a vibronic component of X_2 that would be stabilized for 450 fs by a phonon bottleneck effect, but this is purely conjectural in the absence of any information on vibrational relaxation of excited states in PDA's. If the energy of the 2A_g state is low enough, fast internal conversion to the ground state can account for the 2 ps lifetime.^{30,31} Yet another possibility that cannot be excluded at the present stage is that X_2 results from self-trapping of X_1 . This STE would have to be different from Y since the PA is different. The corresponding self-trapping rate constant would then be $\sim 2 \times 10^{12} \text{ sec}^{-1}$, comparable to the rate of formation of the Y state from the 1B_u free exciton. The slow processes in energy relaxation would then be the decays of the two different self-trapped excitons in 2 and 30 ps, respectively. Since it has been found that PB efficiencies of X_1 and X_2 are comparable, this would imply that the self-trapped exciton X_2 is not drastically different from the corresponding free-exciton X_1 , suggesting weak self-trapping.¹⁹

Nevertheless, as discussed in Sec. IV B above, it cannot be excluded from experimental evidence that Y is formed from X_2 . This would require that X_2 is a free- A_g exciton. Self-trapping into Y would now occur with a rate constant of $\sim 8 \pm 4 \times 10^{10} \text{ sec}^{-1}$. If self-trapping from the 1B_u free exciton occurs at a comparable rate, it is then much too slow to compete with internal conversion into an A_g state.

Further experiments, in particular two-photon absorption spectroscopy would help to confirm the nature of the observed intermediate states.

E. Comparison with bulk PDA results

The results obtained here on isolated PDA chains can be compared to those in the literature on bulk PDA's, at least those showing an exciton absorption around 2 eV (i.e., the so-called "blue" phase). An important difference is that fluorescence from the free exciton is observed in isolated chains^{8,9} whereas it is barely detectable in the blue phase of bulk PDA's.³⁵ Thus, it is clear that some differences exist in the energy-relaxation scheme.

In bulk PDA's, a 2 ps decay time is always present, and a faster decay at short times is sometimes observed. However, a long-lived component has not been reported. The rise time of the PB (or some signal equivalent to it²⁴) is very fast, usually instrument limited, and the decay is exponential, in some experiments over two orders of magnitude, with a time constant of $\sim 2 \text{ ps}$. In bulk PDA-3BCMU and -4BCMU there is no faster component, but an initial decay with $\tau \sim 500 \text{ fs}$ has been observed in Langmuir-Blodgett films of some PDA's.¹² Upon pumping on or near the exciton absorption, PA is observed in a wide spectral range, with different time dependences in the near IR and close to ν_0 . At the longer wavelengths, it appears instantaneously and decays on a sub-ps time scale; at shorter wavelengths, it shows a distinct rise time in the sub-ps range and decays with a time constant of $\sim 2 \text{ ps}$.¹⁶ Kobayashi¹⁶ interprets this observation as a shift of the PA towards higher energies during the first fraction of a ps. This is attributed to the PA by the hot STE during its thermalization, the final PA being that of the relaxed STE which disappears in 2 ps. In this model, hot and thermalized STE's have the same PB efficiency.

Thus, the two short decay times have been observed in bulk PDA's as well. However, in our case we can assign the shorter time to a defined state, since the observed PA can be divided in two distinct spectral regions, each with its own time dependence independent of wavelength after correction for chirp effects.

A longer-lived component is sometimes reported and usually assigned to triplet excitons. We have shown that the triplets formed during singlet exciton relaxation can account for only a small fraction (a few percent) of the total long-lived PB, so that there must be another long-lived state in the gap. In most cases a long-lived component is not reported in bulk PDA's. When the 2 ps decay can be followed over almost two orders of magnitude,²⁴ any contribution of a slow decay cannot exceed 1%. This difference can be explained in the scheme proposed above if internal conversion is faster in bulk PDA's and/or if the self-trapping rate is smaller. The former would also account for the absence of fluorescence in bulk PDA's. However, a long-lived component has been observed on a bulk PDA in conditions where according to the authors, triplet states are not formed.³⁶ In a recent letter,^{20(b)} a decay time of 11 ± 5 ps has been found to be required to account for the time dependence of PA at 1.48 eV upon pumping at 2.0 eV in an oriented film of the PDA poly-DCH. The authors assign this decay time to PA by unthermalized triplet excitons, implying that hot-triplet vibrational relaxation requires ~ 10 ps. This explanation cannot account for our observations for two reasons. First, the study of TT^* absorption in isolated PDA chains reported in our previous paper¹¹ shows that there is no delayed increase of that absorption. Second, it was shown here, as discussed above in Sec. IV C, that there are not enough triplets formed to account for the "long-lived" PB component.

Instantaneous self-trapping as predicted in theoretical 1D models¹⁷ is not observed in isolated chains, despite the fact that electronic states of the chain, as well as the double- and triple-bond stretching vibrations, are strictly 1D. In fact, our results suggest that self-trapping is at best a minor component of exciton relaxation in PDA isolated chains. Bulk PDA's should correspond even less to the theoretical 1D case. The occurrence of self-trapping seems to remain an open question in PDA's.

V. CONCLUSION

This paper deals with nonradiative singlet 1B_u exciton relaxation in isolated PDA chains. Two PA bands originating from two short-lived states are observed. From their respective time dependences, it is concluded here that these two states decay in series in the same relaxation pathway. They have very similar PA cross sections and PB efficiencies. A slowly decaying PB component indicates the existence of a third longer-lived state. It is shown that this state cannot be the triplet 3B_u exciton, and only a fraction of the 1B_u exciton relaxation occurs via this state. Thus, three excited states lie in the optical gap apart from the triplet state. A relaxation scheme is proposed, involving two A_g states in series. It is also concluded that self-trapping, if present, cannot be instantaneous.

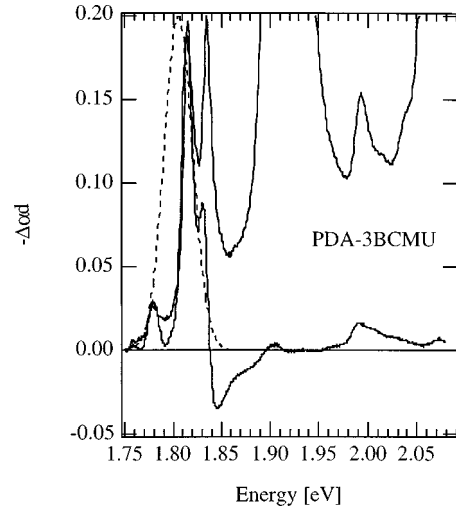


FIG. 12. Differential absorption spectrum of PDA-3BCMU chains (thick solid line). The pump spectrum is shown as the thin dashed line. The linear absorption of the same sample is shown as the thin solid line.

ACKNOWLEDGMENTS

We are very grateful to J. Berréhar for preparing and characterizing the high-quality crystals used in this work. We would also like to thank D. Hulin for fruitful discussions, and A. Alexandrou, J. P. Likforman, and G. Rey for their assistance in the experiments. We gratefully acknowledge support from the French Ministère des Affaires Etrangères for B. Kraabel.

APPENDIX

It was shown elsewhere that the weaker absorption lines on the low-energy side of ν_0 have ground-state configurations different from that of ν_0 ,^{6,8} and that the corresponding transitions show no transfer of oscillator strength to ν_0 (as detected by electroabsorption experiments), and are thus not coupled to it.⁷ They behave exactly as ν_0 in electroabsorption, exhibiting the same Stark shift. This is interpreted in terms of excitons on chains with slightly different conformations and subsequently modified electronic properties. The dominant chain population corresponds to an exciton transition at ν_0 , and ν_a , ν_b , etc. are the exciton transitions of minority chain populations. The ratio of absorption intensities of the respective lines give an approximate idea of the corresponding concentrations. The chain populations corresponding to excitons ν_a and ν_b are always 20–30 times smaller than ν_0 , and even less for ν_c in PDA-3BCMU. A possible explanation is that these minority populations are in the vicinity of stacking faults: PDA-3BCMU and -4BCMU are lamellar crystals.

The present pump-probe experiments yield further information on these transitions, and give an additional argument in favor of the above interpretation.

First, it is possible to pump selectively one of the minority transitions. This is shown in Fig. 12 where the pump is centered on ν_b at 1.81 eV in 3BCMU, overlapping ν_a (1.83 eV) and ν_c (1.78 eV) only slightly, and not at all ν_0 at 1.90 eV. In this case there is *no* bleaching at ν_0 . The very small signal there is also present at negative delay times and is thus as-

sociated to pump diffusion. This shows that the ground states of ν_b and ν_0 do not communicate, further supporting the assumption that they are located on geometrically separate parts of the sample, i.e., on separate chains.

Two PB peaks at 1.99 and 2.07 eV are also seen in Fig. 12. They correspond to the vibronic transitions of ν_b associated to the double-bond stretch (at 1440 cm^{-1}) and the triple-bond stretch (at 2100 cm^{-1}). Their positions and intensities relative to the ν_b PB peak indicate that the exciton transition corresponding to ν_b has Franck-Condon factors and vibrational energies very similar to those of the main exciton at ν_0 . The two small humps at 1.965 and 2.020 eV most probably correspond to the double-bond vibronic bands of ν_c and ν_a , respectively, which are slightly bleached by the pump.

Consequently, ν_a , ν_b , and ν_c are not part of the relaxation pathway of ν_0 . They do not correspond to the states labeled X_1 , X_2 , and Y above.

The time dependence of the 1.99 eV PB peak generated upon pumping at ν_b could be measured up to a delay time of ~ 5 ps. It shows an instantaneous rise and an exponential decay with a time constant $\tau = 1.8 \pm 0.1$ ps. Thus, ν_b behaves very similar to ν_0 . Indeed, Fig. 12 also shows that pumping at ν_b generates a PA band between 1.75 and 2.1 eV very similar to the one generated upon pumping in the ν_0 absorption. In such pumping conditions, the PB signal is too small to allow studying a possible long-lived component, but this is present as well, as shown by the following observation.

The PB peaks at 1.99 and 2.07 eV in Fig. 12 show that vibronic absorption associated to ν_b is present underneath the vibronic absorption spectrum of ν_0 . Therefore, pumping above ν_0 will also produce a PB of ν_b (and ν_a , ν_c as well). This is clearly shown in Fig. 1. Since all these states are distinct and uncoupled, each PB band will decay independently with its own time dependence, and it is found that

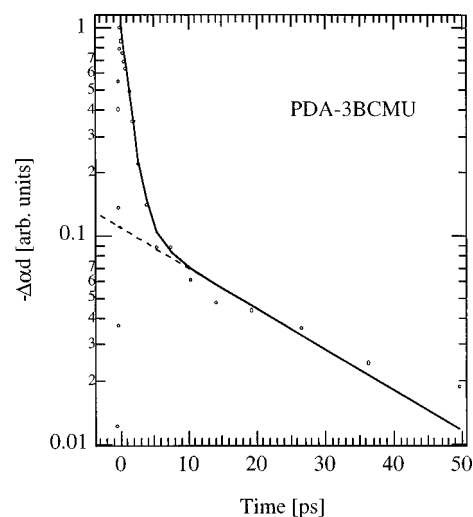


FIG. 13. Time dependence of the PB of ν_b in PDA-3BCMU chains upon pumping at 2.07 eV. The thin solid line is a double exponential fit with time constants of $\tau_2 \approx 1.7$ ps and $\tau_3 = 30$ ps. The thin dashed line shows the contribution of the long-lived component extrapolated to time zero.

they are all very similar. Fig. 13 for instance, corresponds to the PB kinetics of ν_b in PDA-3BCMU, upon pumping at 2.07 eV. The decay is well fitted by a double exponential with $\tau_1 = 1.8 \pm 0.1$ ps and $\tau_2 \sim 30$ ps, and the zero time ordinate ratio of the two components is ~ 10 . Thus, all 1B_u exciton states, though on different types of chains with slightly different transition energies and ground-state geometries, have similar energy relaxation pathways. At least, states X_2 and Y are present with similar lifetimes. The free-exciton lifetimes and the existence of an X_1 state related to the minor chain populations have not been studied directly.

*Present address: Los Alamos National Laboratories, MS J585, Los Alamos, NM 87545.

†Also at IUFM de l'Académie de Créteil, 94861 Bonneuil-sur-Marne Cedex, France.

‡Author to whom correspondence should be addressed. Electronic address: schott@gps.jussieu.fr

¹M. Schott and G. Wegner, in *Nonlinear Optical Properties of Organic Molecules and Crystals*, edited by D. S. Chemla and J. Zyss (Academic, Orlando, 1987), Vol. II, p. 1.

²*Polydiacetylenes*, edited by D. Bloor and R. R. Chance (Martinus Nijhoff, Dordrecht, 1985).

³Adv. Polym. Sci. **63** (1984), edited by H. J. Cantow.

⁴M. Yan, L. J. Rothberg, E. W. Kwok, and T. M. Miller, Phys. Rev. Lett. **75**, 1992 (1995).

⁵J. W. P. Hsu, M. Yan, T. M. Jedju, and L. J. Rothberg, Phys. Rev. B **49**, 712 (1993).

⁶S. Spagnoli, J. Berréhar, C. Lapersonne-Meyer, M. Schott, A. Rameau, and M. Rawiso, Macromolecules **29**, 5615 (1996).

⁷A. Horvath, G. Weiser, C. Lapersonne-Meyer, M. Schott, and S. Spagnoli, Phys. Rev. B **53**, 13 507 (1996).

⁸C. Lapersonne-Meyer, J. Berréhar, M. Schott, and S. Spagnoli, Mol. Cryst. Liq. Cryst. Sci. Technol., Sect. A **256**, 423 (1994).

⁹S. Spagnoli, J. Berréhar, C. Lapersonne-Meyer, and M. Schott, J. Chem. Phys. **100**, 6195 (1994).

¹⁰S. Haacke, G. R. Hayes, C. Lapersonne-Meyer, and M. Schott (unpublished).

¹¹B. Kraabel, D. Hulin, C. Aslangul, C. Lapersonne-Meyer, and M. Schott, Chem. Phys. **227**, 83 (1998).

¹²M. Yoshizawa, K. Nishiyama, M. Fujihira, and T. Kobayashi, Chem. Phys. Lett. **207**, 461 (1993).

¹³T. Kobayashi, M. Yoshizawa, U. Stamm, M. Taiji, and M. Hasegawa, J. Opt. Soc. Am. B **7**, 1558 (1990).

¹⁴M. Yoshizawa, A. Yasuda, and T. Kobayashi, Appl. Phys. B: Photophys. Laser Chem. **53**, 296 (1991).

¹⁵T. Kobayashi, in *Relaxation in Polymers*, edited by T. Kobayashi (World Scientific, Singapore, 1996), p. 1.

¹⁶T. Kobayashi, Synth. Met. **54**, 75 (1993).

¹⁷E. I. Rashba, in *Excitons-Selected Chapters*, edited by E. I. Rashba and M. D. Sturge (North-Holland, Amsterdam, 1987), p. 273.

¹⁸E. I. Rashba, Synth. Met. **64**, 255 (1994).

¹⁹H. Sumi and A. Sumi, J. Phys. Soc. Jpn. **63**, 637 (1994).

²⁰(a) T. Kobayashi, M. Yasuda, S. Okada, H. Matsuda, and H. Nakanishi, Chem. Phys. Lett. **267**, 472 (1997); (b) J. Kinugasa, S. Shimada, H. Matsuda, H. Nakanishi, and T. Kobayashi, *ibid.* **287**, 639 (1998).

²¹V. Klimov and D. McBranch, Opt. Lett. **23**, 277 (1998).

²²T. F. Albrecht, K. Seibert, and H. Kurz, Opt. Commun. **84**, 223 (1991).

²³M. Joffre, D. Hulin, A. Migus, A. Antonetti, C. Benoit à la Guillaume, N. Peyghambarian, M. Lindberg, and S. W. Koch, Opt. Lett. **13**, 276 (1988).

- ²⁴B. I. Greene, J. Orenstein, R. R. Millard, and L. R. Williams, *Phys. Rev. Lett.* **58**, 2750 (1987).
- ²⁵S. Suhai, *J. Chem. Phys.* **85**, 611 (1986).
- ²⁶C. Jundt, G. Klein, and J. L. Moigne, *Chem. Phys. Lett.* **203**, 37 (1993).
- ²⁷J. M. Leng, Z. V. Vardeny, B. A. Hooper, K. D. Straub, J. M. J. Madey, and G. L. Baker, *Mol. Cryst. Liq. Cryst. Sci. Technol., Sect. A* **256**, 617 (1994).
- ²⁸B. Lawrence, W. E. Torruellas, M. Cha, M. L. Sundheimer, and G. I. Stegeman, *Phys. Rev. Lett.* **73**, 597 (1994).
- ²⁹W. A. Yee, R. H. O'Neil, J. W. Lewis, J. Z. Zhang, and D. S. Klinger, *Chem. Phys. Lett.* **276**, 430 (1997).
- ³⁰P. O. Anderson, S. M. Bachilo, R.-L. Chen, and T. Gillbro, *J. Phys. Chem.* **99**, 16 199 (1995).
- ³¹M. Mimuro, S. Akimoto, S. Takaichi, and I. Yamazaki, *J. Am. Chem. Soc.* **119**, 1452 (1997).
- ³²B. S. Hudson, B. E. Kohler, and K. Schulten, *Excited States*, edited by E. C. Lim (Academic, New York, 1982), Vol. 6, p. 1.
- ³³P. Tavan and K. Schulten, *Phys. Rev. B* **36**, 4337 (1987).
- ³⁴F. Guo, D. Guo, and S. Mazumdar, *Phys. Rev. B* **49**, 10 102 (1994).
- ³⁵A. Yasuda, M. Yoshizawa, and T. Kobayashi, *Chem. Phys. Lett.* **209**, 281 (1993).
- ³⁶S. Molyneux, A. K. Kar, B. S. Wherrett, T. L. Axon, and D. Bloor, *Opt. Lett.* **18**, 2093 (1993).